Mechanism of MgO–C refractories corrosion interacting with $CaO–MgO–Al_2O_3–SiO_2–FeO$ slags

I. A. Krasnyanskaya*, Cand. Eng., Head of the Laboratory of Complex Chemical Researches* [1]*, N. P. Lyakishev Scientific Center for Complex Processing of Raw Materials, iakrsn@gmail.com;*
K. N. Anisimov*, Cand. Eng., Head of the Laboratory of Refractory Materials* [1]*;*
M. P. Gusev*, Cand. Eng., Chief Business Development Officer* [2]*;*
M. G. Moshchenko*, Cand. Eng., Head of the Programs, Directorate of Researches and Developments* [3]*;*
D. V. Karavaev*, Engineer, Directorate of Researches and Developments* [3]

[1] *I. P. Bardin Central Research Institute of Ferrous Metallurgy (Moscow, Russia)*
[2] *LLC "Cyberphysics" (Moscow, Russia)*
[3] *PAO NLMK (Lipetsk, Russia)*

** Corresponding author, iakrsn@gmail.com*

A. I. Volkov took part in the work

In the production of ultra-low carbon steels, it is especially important to prevent the carburization of the melt. The latter can occur as a result of lining corrosion, when carbon ions transfer from the ladle lining to the melted steel. This process is mainly caused by the corrosive effect of slags on the refractory and is associated with their chemical composition and physical properties, such as viscosity. While many slag-refractory systems are currently used in the steel making, such systems often lack sufficient data for the strict modeling of the interaction process. In this work, we investigate the corrosive behavior of various slags on MgO–C lining in order to minimize the increase in carbon during the dynamo steel production. It is established that the main factor influencing the wear of the lining is its phase composition. Spinel, which forms at the slag-refractory interface, can be washed out from the boundaries of the lining, exposing its internal layers to the slag. However, in the presence of calcium aluminate $CaAl_4O_7$ in the remaining melt, the intensive washout of the spinel layers is inhibited. These components act as a protective factor even when MgO content in the slag is relatively low. Thus, by changing the composition of the slag, it is possible to obtain extremely low wear of MgO–C refractories even with small MgO content in the slag and therefore reduce the subsequent carburization of the metal caused by corrosion of the refractories in the slag zone.
Key words: periclase, MgO–C refractories, spinel, calcium aluminate, refractory corrosion, slag, phase composition, dynamo steel.
DOI: 10.17580/cisisr.2024.01.04

Introduction

During the production of dynamo steel the technology of RH-process is typically used to reduce the content of dissolved oxygen and carbon in the melt. In the process of evacuation, silicon in the form of ferrosilicon and aluminum are supplied as deoxidizers and alloying agents into the ladle equipped with MgO–C refractory for the slag zone. It is noted that the addition of silicon and aluminum increases the carbon content in steel in an amount that cannot be explained by the carbon content in the deoxidizers and alloying agents alone. In addition, with subsequent secondary refining, the carbon content increases. Thus, the present study focuses on the reasons for the carbon increase, which are attributed to the slag influence. The goal of the paper is to evaluate the slag parameters that prevent the refractory wear and subsequent dissolution of carbon in the melted steel.

Thus far, the investigation of MgO–C refractory destruction under the slag influence was discussed in many works [1–10]. In general, the mechanism of refractory corrosion and carburization of metal can be explained in the following way:

1. Oxidation of carbon at the slag-lining interface;
2. Penetration of the slag melt into the refractory;
3. Exposure of all new carbon-containing layers of the refractory material;
4. Ingress of the carbon at the slag-metal interface and its dissolution in steel.

Apart from the lining corrosion, the increase in the carbon content of metal can be influenced by other factors. For example, when using carbon-containing magnesia refractory, gasification of carbon in MgO–C refractories can occur by direct interaction of lining carbon and oxygen in the reactor atmosphere or by MgO reduction with carbon at high temperatures (more than 1400 °C) [11,12]:

$$2C(s) + O_2(g) = 2CO(g) \quad (1)$$

$$C(s) + MgO(s) = Mg(g) + CO(g) \quad (2)$$

Carbon monoxide formed by these reactions can then be reduced by aluminum dissolved in steel by the reaction [6]:

$$2[Al] + 3CO(g) = (Al_2O_3) + 3[C] \quad (3)$$

For the steel grade under study (dynamo steel), this process can be especially relevant, since it contains high concentrations of Al, although an increase is observed after the addition of not only aluminum, but also ferrosilicon.

Also, worth noting the carbon solubility decrease in the slag with a change in its composition. Indeed, it is difficult to imagine that the carbon in the oxide melt remains bound and is not transferred into the gas phase in the form of CO_2. Nevertheless, some studies [13–17] suggest that the solubility of carbon in oxide melts is nonzero, and variation of the slag composition by adding alloying and deoxidizing agents can change this solubility, thus intensifying the transition of carbon from slag to metal.

The factors that protect the lining from the corrosive effects of slag are explored further.

Formation of a protective layer. According to some researchers, a protective layer of hard-melting complex oxides can form in the zone of contact between the slag and the lining [9,18,19]. In [19] a scheme was proposed, in which the interaction of MgO–C lining with slag has the following sequence:

1. Reduction reaction between FeO in the slag and carbon in MgO–C refractories with forming of a foamy slag, metallic Fe and voids in the refractory;
2. Slag penetrating into these voids after decarburization on the surface;
3. Interaction of penetrated slag with MgO particles and forming a high melting point protection layer.

However, not all slags are suitable for creating a protective layer [20].

Slag saturation with the main component of refractory. Slag saturated with MgO does not have a corrosive effect on the magnesia lining, since in such solution a solid oxide phase precipitates instead. Achieving the required MgO concentrations in the entire volume of the slag is difficult for technological reasons. However, if there are pores in the lining material, in which the slag can be retained, it is possible to locally obtain a solution with a high concentration of MgO, which ensures the formation of a protective layer [9, 21].

High viscosity of the slags. High viscosity prevents the slag penetration into cracks and pores of the lining [9, 21]. However, its effect on corrosion can be ambiguous. On the one hand, the lower the viscosity is, the more intense the chemical interaction at the interface becomes – the slag flows into the cracks and voids between the structural components of the refractory and washes them out. On the other hand, in the case of the formation of a protective layer, the liquid slag can provide better adhesion to the lining surface, by flowing between the refractory grains, as shown in [20].

Despite a large number of works devoted to the interaction between slag and magnesia lining, this process is influenced by many factors, and there is no detailed study that would take into account all of them at once. In particular, most studies are limited to the content of Al_2O_3 in the investigated slags in the region of 20%, while for dynamo steel this content at the end of evacuation can exceed 30 %. Other research focuses on the effects of additives such as CaF_2 and does not cover a wide range of compositions. The methodology of experiments vary as well: the method of static determination for slag resistance; dynamic methods in an induction furnace with a melt placed in a magnesia crucible [22]; the "rotating finger" method, in which a refractory sample on a rotating holder is immersed in the melt and then rotated [23–26]. Refractory samples in these works have all different compositions, so it is challenging to make an appropriate comparison.

In order to obtain better insight in the corrosion process that occurs during the industrial steelmaking, we consider the slags with a wide range of chemical compositions, which can form during the dynamo steel processing. Likewise, we use lining samples made from MgO–C refractories, similar to ones implemented in the production. Thus, we aim to simulate the real conditions o of the technological process, so the obtained results would be suitable for the operating industrial plant.

The paper is organized as follows: first, we describe the samples preparation, then provide details on the conducted experiments and, at last, discuss the obtained results. The paper ends with a conclusion section and briefly outlines the further possible research.

Experimental and Analysis Method

A series of high-temperature experiments were carried out at 1550 °C under a well-controlled inert atmosphere. Slags were preliminarily synthesized by mixing a desired proportion of pure chemical reagents, wt %: CaO (> 99.5), MgO (> 99.7), Al_2O_3 (> 99.0), SiO_2 (>99.5), FeO (> 99.5). They were melted in ZrO_2 crucibles in a heating furnace above 1500 °C. After the melting and cooling, the crucibles were crushed, slag was separated from the supporting material and milled in the grinding pan. The slag compositions were designed to simulate those obtained in the industrial conditions. All investigated chemical compositions are presented in **Table 1**.

Hot-rolled dynamo steel sheets provided by an industrial partner were cut on a band-saw and degreased. The composition of the metal is shown in **Table 2**.

Refractory samples were cut from periclase-carbon bricks using a core extractor. Each sample had length of 200 mm and the diameter of 13 mm. Refractory characteristics are presented in **Table 3**.

The slags and metal prepared in this way were then used in an experiment carried out by the "rotating finger" method in a heating furnace, the scheme of which is shown

Table1. **Slag composition (wt%)**

Composition	Al_2O_3	FeO	CaO	MgO	SiO_2
1	9.5	15.2	59.0	6.0	5.5
2	31.9	16.5	38.0	5.6	5.7
3	5.5	17.4	45.2	5.8	22.2
4	27.8	17.4	25.5	5.7	21.5
5	5.5	17.7	42.5	16.3	14.0
6	30.5	17.1	30.4	16.1	5.6
7	10.3	17.1	34.4	15.0	21.5
8	27.8	17.7	16.1	16.1	21.5
9	9.7	17.9	46.5	9.1	12.4
10	25.5	17.5	27.9	12.7	14.1
11	19.6	18.1	44.2	8.6	5.0
12	13.7	17.6	31.1	12.9	23.1
13	22.7	16.2	39.6	6.8	13.6
14	15.5	16.5	32.1	19.6	14.6
15	10.8	17.7	50.6	5.4	11.1
16	14.6	17.2	35.5	13.1	17.9

Table 2. **The chemical composition of the dynamo steel (wt%)**

Al	Si	Mn	C	Fe
1.0	3.0	0.15	0.002	balance

Table 3. **Refractory specimen characteristics**

MgO, wt%	C, wt%	Apparent density, g/cm³	Effective porosity, %
≥92	≥8	≥2.8	≤9

in **Fig. 1.** Steel in an amount of 800 g was placed in a ZrO_2 crucible and heated in a tubular furnace at a rate of 10 °C/min with a continuous flow of argon (> 99.999 wt%) into the oven chamber. After the steel melted and reached a temperature of 1873 K, 50 g of the prepared slag was placed on the metal through a corundum tube. After the slag was melted, the refractory sample was immersed in the metal on a depth of 20 mm and rotation was started at a speed of 100 rpm. During the experiment, samples of metal and slag were taken with a quartz sampler. After 60 minutes, the rotation was stopped, the refractory sample was taken out of the melt and cooled in air. The crucible with the melt was cooled together with the furnace.

To assess corrosion, refractory samples were prepared on a RotoPol 35 grinding and polishing machine with a PmdForce 20 sample holder (Struers), after which they were filled with epoxy resin under vacuum on an impregnator for cold pressing of samples (CitoVac, Struers).

The sample structure with the determination of its chemical composition after experiments was investigated on the mineralogical complex MLA System Quanta 650 (FEI Company). This complex includes a SEM Quanta 650 scanning electron microscope, an EDAX Silicon Drift Detectors controlled by Genesis software, and an integrated MLA Suite software. Before examination on a scanning electron microscope, carbon spraying was applied to the specimens to ensure conductivity.

The analysis of the chemical composition of the slags was carried out on an AXIOSmaxAdvanced X-ray fluorescence spectrometer (PANalytical, Netherlands). The carbon content in the metal and slag was determined on an analyzer for sulfur, total carbon and carbonate CS-2000 (Eltra, Germany).

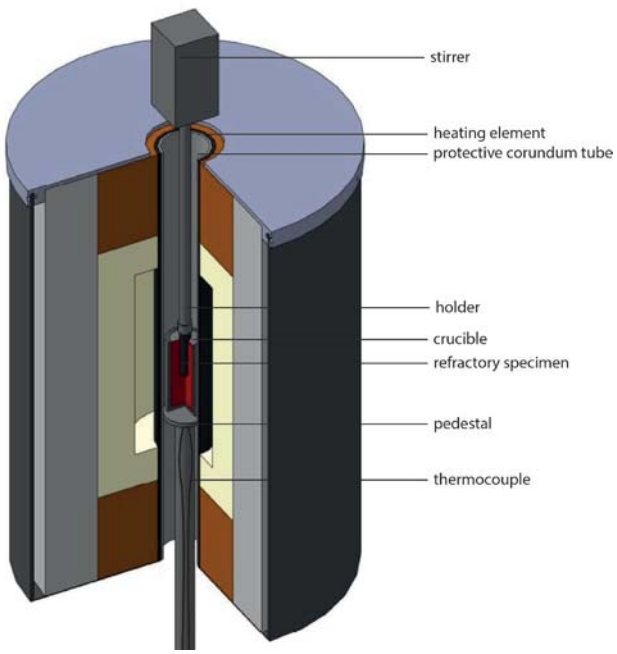

Fig. 1. Schematic diagram of the experimental apparatus

Results and discussion

One of the obtained experiment samples (slag 8) is shown in **Fig. 2**. It features general view and the magnified slag interaction section.

(*a*) (*b*)

Fig. 2. Experiment sample (*a*) and its slag zone longitude section (*b*) (slag 8)

in industrial conditions. The content of Al_2O_3 in industrial slags reaches 40–50 wt%. During smelting, dissolved in the metal Al reduces FeO in the slag. Hence, in the following experiments, FeO is absent and an additional amount of Al_2O_3 is dissolved in it. The wear of refractories was estimated

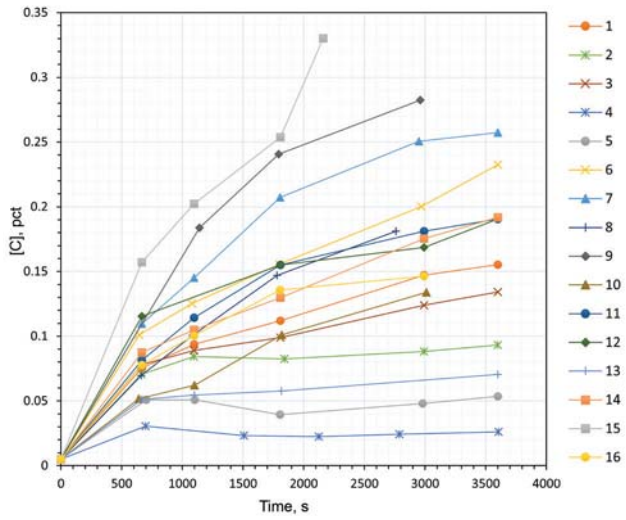

Fig. 3. Carbon content increase in steel during the experiment

Each specimen demonstrates a sharp increase of carbon content in steel (**Fig. 3**), which is associated with the metal carburization from the sample surface. The smallest increase in steel carbon corresponds to slags 4, 5, 13, 2. The largest increase is found for slags 9, 15. The final slag chemical compositions are shown in the **Table 4**. After comparison Tables 1 and 4, it can be seen that the slag final composition changes towards an increase in Al_2O_3, which is also observed by the area of corrosion in photographs of longitudinal sections (**Fig. 2b**) in the JMicroVision software [27]. Viscosity and limiting solubility of MgO in slags were calculated using the FactSage program [28]. The red lines in Fig. 2b indicate the original boundaries of the specimen. Comparison of the corrosion degree of the samples and the increase in carbon in the metal is shown in **Fig. 4**. It can be seen that the increase in carbon is directly proportional to the corrosion degree,

Table 4. **Final chemical composition of slags**

Slag	Al_2O_3	FeO	CaO	MgO	SiO_2	C
1	48.54	1.33	37.43	6.45	3.24	0.15
2	64.53	0.90	23.43	4.85	3.41	0.09
3	61.65	0.30	19.84	5.76	6.65	0.13
4	53.10	6.08	27.59	3.71	11.28	0.02
5	27.75	3.97	38.62	13.79	16.12	0.05
6	59.40	1.57	18.21	18.01	3.05	0.23
7	54.30	1.45	15.23	17.50	10.34	0.25
8	47.78	4.97	13.23	22.50	12.50	0.18
9	49.60	2.13	17.08	23.10	8.06	0.28
10	56.30	2.22	16.22	22.05	5.78	0.13
11	62.72	0.65	22.97	9.94	3.42	0.19
12	59.05	1.59	15.07	18.08	6.88	0.19
13	61.76	1.00	21.38	5.17	6.99	0.07
14	60.65	2.42	17.76	14.70	5.02	0.19
15	48.14	0.56	27.31	12.83	6.25	0.33
16	56.60	1.17	12.42	26.34	3.28	0.14

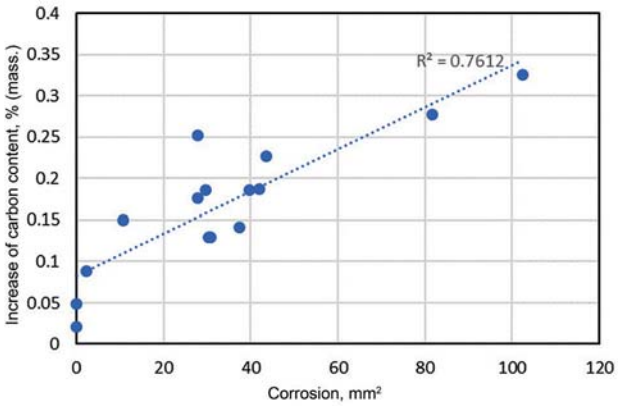

Fig. 4. Dependence of carbon increment in steel on lining corrosion

which indicates that the refractory wear is undoubtedly the main factor leading to the carburization of metal. At the same time, other factors, such as the change in the solubility of carbon in the slag (which depends on its composition) and the reaction mechanism (3), have minimum impact.

The results of corrosion and carbon increase in steel do not correlate directly with any single input parameter. **Fig. 5** shows that there is no direct relationship between the content of Al_2O_3, MgO in the slag, basicity, viscosity and limiting solubility of MgO. Basicity was calculated using the formula $B = (CaO + MgO) / (SiO_2 + Al_2O_3)$. For slags with the greatest corrosion (compositions 9 and 15), the lowest viscosity was obtained, which can explain their high corrosion effect on the lining (Fig. 5*d*).

The obtained results can be conditionally divided into three groups (Fig. 5*c*). For slags 1, 2, 4, 5, 13, corrosion, as well as an increase in carbon, was insignificant. Slags 9 and 15 showed the highest corrosion. The rest took an intermediate position in their effect on the lining.

The experimental results showed not only the absence of a direct relationship between any single characteristic of the slag (content of a certain component, viscosity, etc.), but also some counterintuitive observations. Namely, in slag 2, the MgO content was low, and it was reasonable to assume that it would be more aggressive towards the periclase refractory material than the compositions more saturated with MgO. However, this composition showed, on the contrary, low corrosion. As can be seen from the data in Fig. 5*e*, at approximately the same value of the solubility of MgO for samples 1, 5, 9, 15, the wear values for 1 and 5 are minimal, and for 9 and 15, they are maximal.

To explain the reasons that intensify or inhibit the erosion of the lining by the slag melt, a micro X-ray spectral analysis of refractory samples in the zone of the slag belt was carried out from three groups: those showing minimal wear (slag 2), medium (slags 6, 8), maximum (slag 15). The results are shown in **Fig. 6–9**. Black areas correspond to pores formed as a result of sample spalling during specimen preparation. The phases of the melted slag were defined by the stoichiometric ratio of the components in the corresponding areas.

First, we note that in the SEM photographs of slag 2 sample, one can see corrosion that was not observed visually. This wear area is highlighted in green. Fig. 6 shows that the

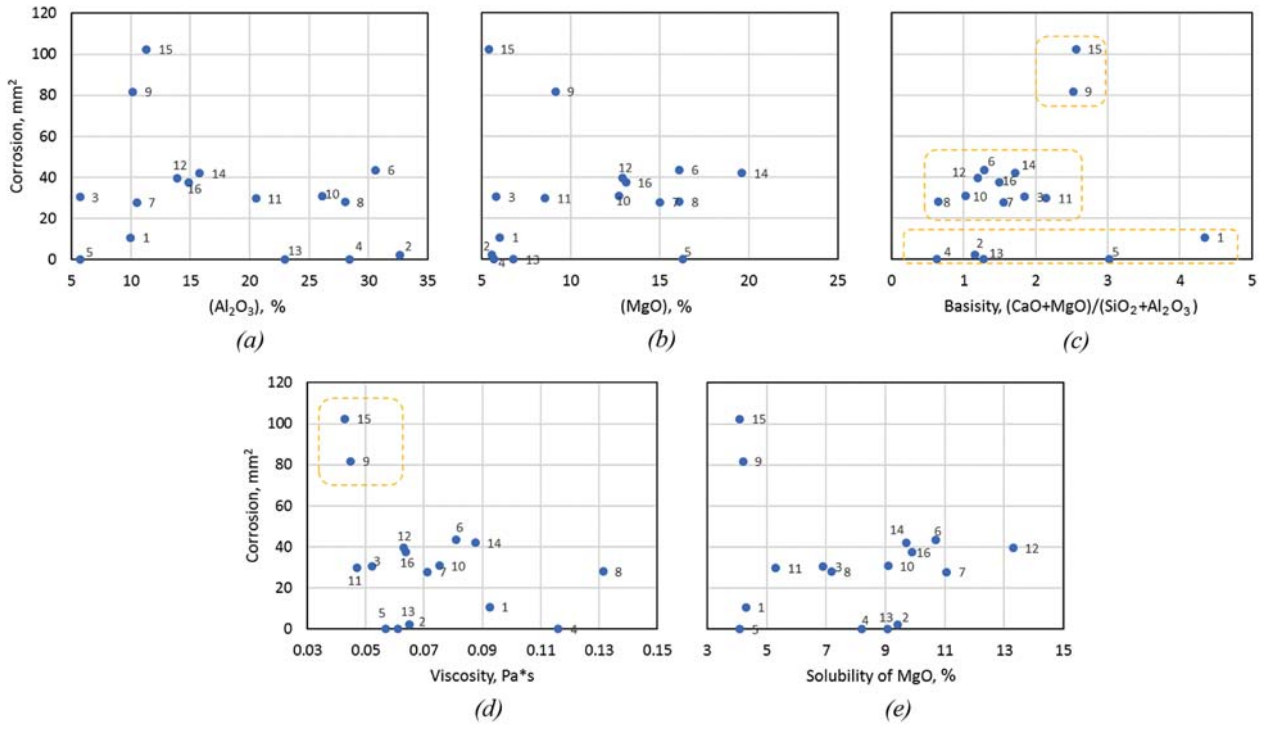

Fig. 5. Dependence of lining wear on various factors: Al_2O_3 content (*a*), MgO content (*b*), basicity (*c*), viscosity (*d*), limiting solubility of MgO (*e*)

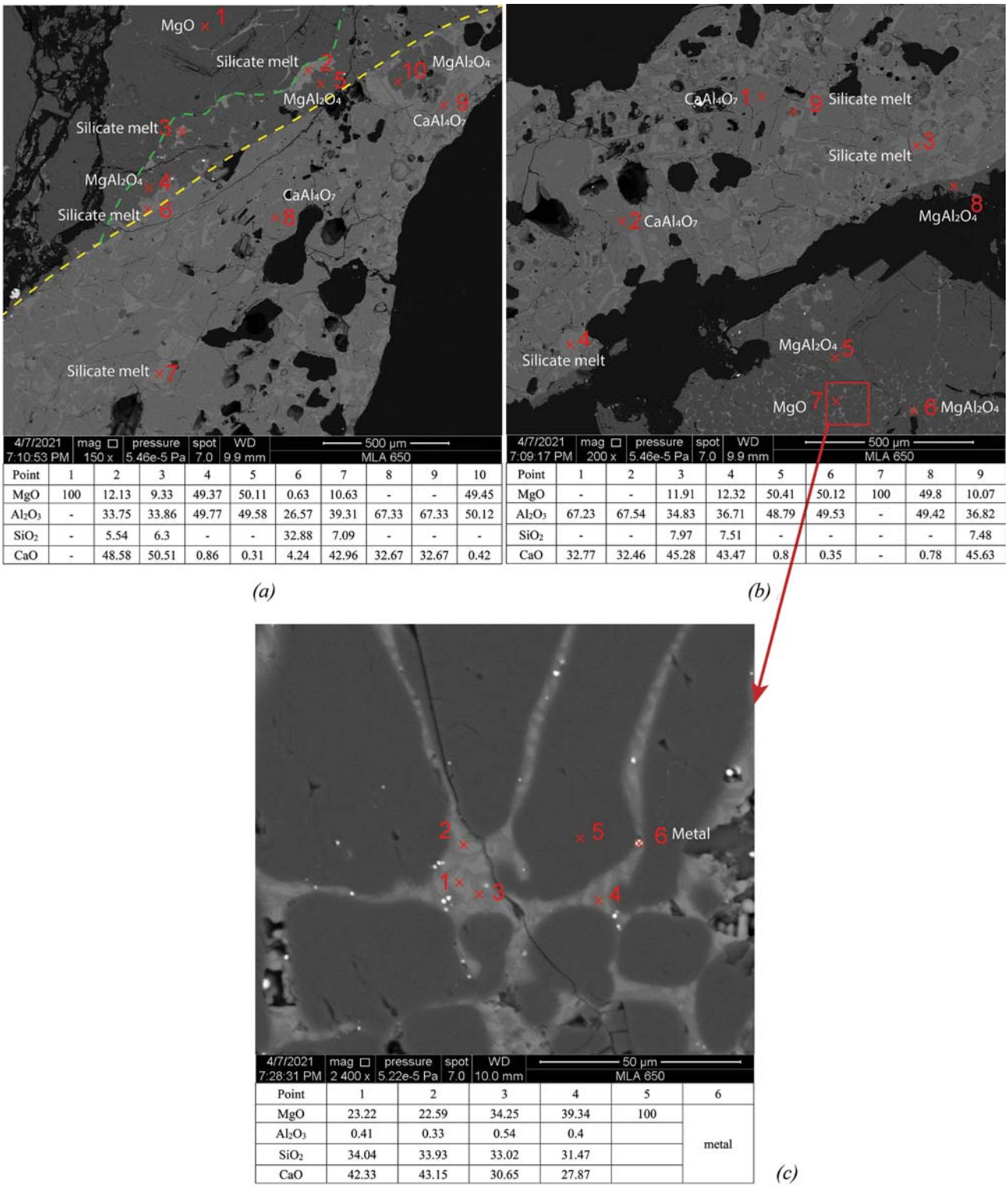

Point	1	2	3	4	5	6	7	8	9	10
MgO	100	12.13	9.33	49.37	50.11	0.63	10.63	-	-	49.45
Al_2O_3	-	33.75	33.86	49.77	49.58	26.57	39.31	67.33	67.33	50.12
SiO_2	-	5.54	6.3	-	-	32.88	7.09	-	-	-
CaO	-	48.58	50.51	0.86	0.31	4.24	42.96	32.67	32.67	0.42

Point	1	2	3	4	5	6	7	8	9
MgO	-	-	11.91	12.32	50.41	50.12	100	49.8	10.07
Al_2O_3	67.23	67.54	34.83	36.71	48.79	49.53	-	49.42	36.82
SiO_2	-	-	7.97	7.51	-	-	-	-	7.48
CaO	32.77	32.46	45.28	43.47	0.8	0.35	-	0.78	45.63

Point	1	2	3	4	5	6
MgO	23.22	22.59	34.25	39.34	100	metal
Al_2O_3	0.41	0.33	0.54	0.4		
SiO_2	34.04	33.93	33.02	31.47		
CaO	42.33	43.15	30.65	27.87		

Fig. 6. X-ray spectral analysis of slag 2 sample: interaction between the slag and refractory (*a*), (*b*) , magnified image of the zone with refractory deep layers and oxide melt between finely dispersed MgO grains (*c*)

silicate melt of oxides MgO, Al_2O_3, CaO, SiO_2 in different ratios (light gray phase in the photo) penetrates into cracks between refractory grains, dissolving MgO. As a result of saturation of the oxide solution with MgO, spinel is formed ($MgAl_2O_4$, highlighted in green), which has a high melting point (more than 2273 K) and crystallizes at experimental temperatures (1873 K). Since the yellow line represents the boundary of the sample, it can be concluded that spinel is formed within the refractory material. First, it remains there, but then it begins to dissolute with the remaining oxide melt, which is especially noticeable in slag samples 6 and 8 (Fig. 7 and 8). For slag sample 2, there is no noticeable washout of the refractory. The precipitation of the spinel crystalline phase from the melt can be judged by the fact that it has

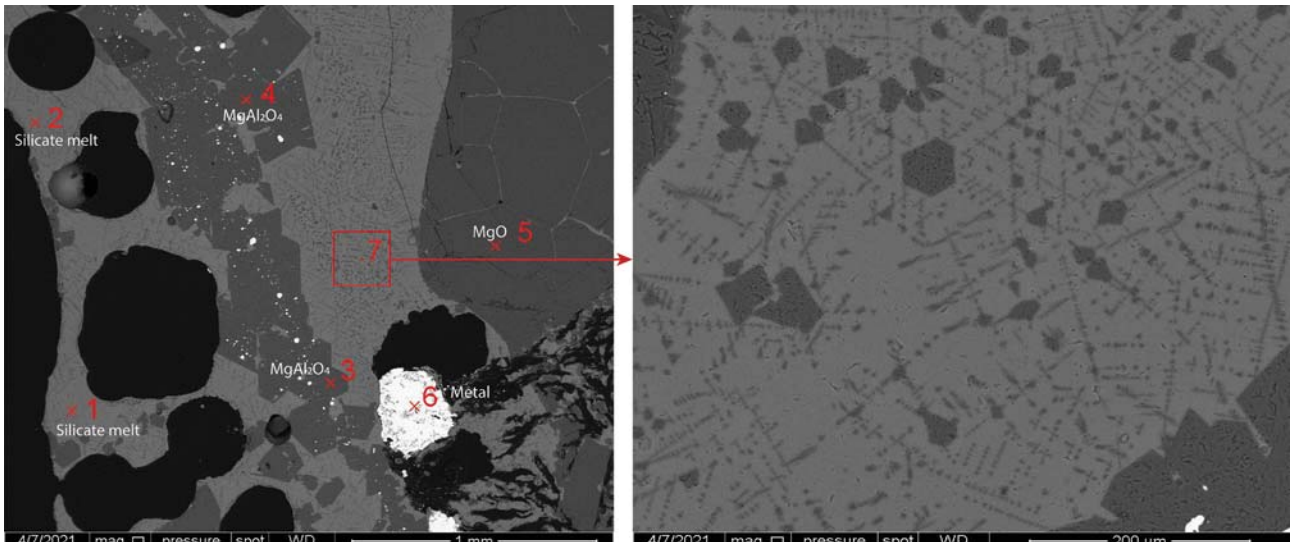

Point	1	2	3	4	5	6
MgO	17.65	16.67	51.03	51.01	100	metal
Al_2O_3	35.11	33.46	48.97	48.99	-	
SiO_2	5.52	6.22	-	-	-	
CaO	41.72	43.65	-	-	-	

Fig. 7. Results of X-ray spectral microanalysis of slag 6: removal of the formed spinel from the refractory surface (*a*), formation of spinel dendrites in the melt (*b*)

a characteristic geometric shape, which is clearly visible in samples 6 and 8 (Fig. 7 and 8), where it is formed in a large amount and is distributed in the oxide melt. Metal droplets are deposited on the surface of the solid MgO phase in the refractory material. These observations are confirmed by analyzing Fig. 7: the edges of the refractory material (point 5) are also blurred, and the metal phases (white spots) are deposited mainly on spinel particles (point 4). This indirectly confirms the assumption that solid spinel particles are formed not during the cooling of the melt, but during the melting process. As a result, metal droplets distributed in the oxide melt are aggregated on the periclase surface. After the spinel particles are separated from the refractory surface, they are carried away by the oxide melt flows to the slag. The Fig. 7b shows how the spinel formation process proceeds in the oxide melt. Dendrite-shaped phases are precipitated in

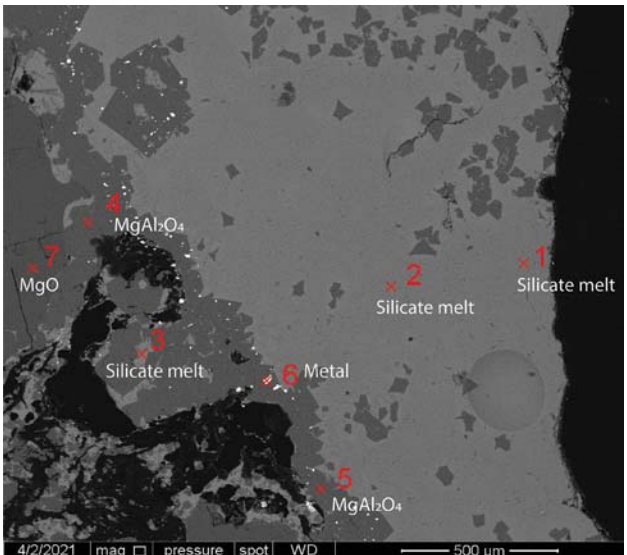

Point	1	2	3	4	5	6	7
MgO	15.15	14.79	15.75	51.11	50.46	metal	100
Al_2O_3	34.97	34.94	21.35	48.89	49.13		-
SiO_2	17.29	17.09	18.79	-	-		-
CaO	32.07	32.71	43.37	-	0.41		-

Fig. 8. Results of X-ray microanalysis of slag 8 sample

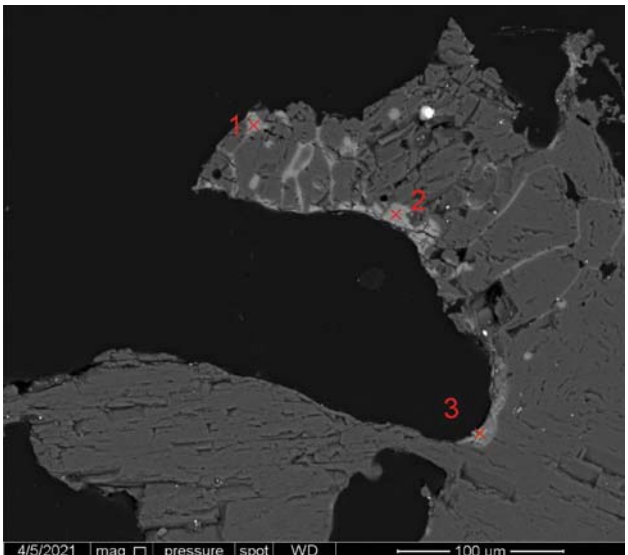

Point	1	2	3
MgO	9.44	10	47.98
Al_2O_3	18.61	17.58	20.66
SiO_2	20.58	23.19	7.86
CaO	49.07	46.86	4.79

Fig. 9. Results of X-ray microanalysis of slag 15 sample

the slag. These dendrites, most likely, represent the initial stage of spinel formation, since their further growth occurs along them", which is clearly visible in the highlighted area in Fig. 7. For sample 2, the presence of calcium dialuminate ($CaAl_4O_7$) in the slag around the refractory is also observed. Its melting point exceeds the experimental temperature, thus one can expect the crystallization during melting at 1600 °C. These inclusions are also crystalline. It can be assumed that for slag 2 it is exactly the phase $CaAl_4O_7$ that prevents the washing out of the spinel formed in the refractory, the further contact of the oxide solution with the refractory MgO and the destruction of the sample. Indeed, although spinel formed in sample 2, it remained within the boundaries of the refractory. For slag sample 15, which belongs to the group of compositions that showed the maximum corrosion, $CaAl_4O_7$ is absent, and the slag is an amorphous phase of silicate melt of complex composition (Fig. 9).

For clinkers based on Al_2O_3 and MgO, the presence of calcium aluminates in the oxide melt is considered by researchers as a protective factor that prevents the destruction of the lining due to the fact that the formation of refractory aluminates such as $CaAl_4O_7$ and $CaAl_{12}O_{19}$ increases the viscosity and the melting point of the slag [29]. Apparently, these phases have a similar effect in the case of the slag melt interaction with the periclase refractory.

It can be concluded that spinel is not a protective structural component of the slag by itself, but depends on the properties of the surrounding solution and its corrosion ability. Indeed, spinel is formed due to the material of the refractory itself, by dissolving MgO and saturating the oxide melt with it. In fact, this is the process of lining corrosion, and in the general case, it continues until the component required for this reaction (here Al_2O_3), is consumed. Indeed, Fig. 6c (points 1–4) shows the composition of the melt flowing deep into the refractory after the spinel formation has already taken place on the surface, which is almost completely free of Al_2O_3. However, if there are factors in the system that inhibit the supply of the necessary reagents to the reaction zone, this process can stop, and the corrosion of the lining will be restricted. This factor can be the properties of the remaining melt – its high viscosity or the formation of other high melting phases in it, which prevent the washing out of the reaction products of the lining and oxide melt. This conclusion is consistent with the fact that, indeed, slag 8 had less wear than slag 6.

It is widely believed that spinel, which forms in the slag during its interaction with the refractory [9] or is present in the refractory composition [30], has a protective effect on the lining. However, the chemical corrosive effect of slag on a lining containing MgO or $MgAl_2O_4$ will primarily depend on the composition of the slag itself. Based on the results of this study, it can be assumed that, since it was spinel that was formed as a result of the slag-lining interaction, then when using refractories containing $MgAl_2O_4$ in their composition, destruction as a result of a chemical reaction would not occur, since during the dissolution of periclase, the slag is saturated with MgO with precipitating of $MgAl_2O_4$. On the other hand, when working with slags, in which the main phase is not spinel, but periclase, there is no thermodynamic stimulus for the dissolution of MgO, and corrosion is restricted by thermodynamics. For such slags, periclase refractories will show higher corrosion resistance.

Regression model development of the MgO–C lining corrosion

As was shown above, it is incorrect to assess the possible degree of lining corrosion based on any separate factor alone, and it is necessary to consider all criteria simultaneously (component content, viscosity, limiting solubility of MgO in slags).

The mutual influence of parameters was calculated according to the sensitivity analysis [31] in a form of correlation matrix (**Fig. 10**). Here, the first 5 factors are the chemical composition of the slag, Visc is the viscosity of the slag calculated in the FactSage program, and Wear is the wear of the lining. Dyn_C is the increase in carbon, which is found as the ratio of the absolute carbon value to the time (during which the experiment was carried out). MgOS is the indicator characterizing the limiting solubility of magnesium, found as:

$$MgOS = (MgOSol - MgO)/MgO, \quad (4)$$

where *MgOSol* is a solubility of magnesium, calculated in the FactSage softwear.

Fig. 10 shows which parameters and in which direction affect the dynamics of carbon growth and lining wear. A direct correlation between the wear and carbon gain is evident, however other parameter relationships are less straightforward. In order to evaluate the values of carbon growth and lining wear, outside the range of the studied slags, two predictive models were built with the input parameters: chemical composition of slags (Al_2O_3, CaO, MgO, SiO_2), viscosity (Visc), limiting solubility MgO (MgOS), and the output parameters: carbon gain (Dyn_C) and liner wear (Wear). FeO was excluded from the input parameters of the models because it linearly depends on the remaining input factors:

$$FeO = 100 - Al_2O_3 - CaO - MgO - SiO_2 \quad (5)$$

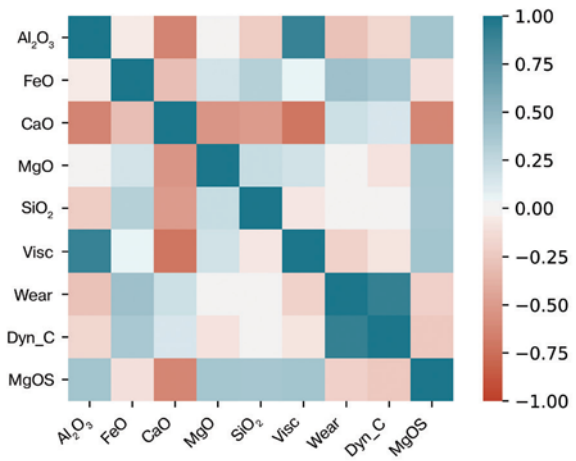

Fig. 10. Correlation matrix

The calculations were made in Python by using standard machine learning libraries [32]. Data was divided into training (80 %) and test (20 %) groups. Several standard models (Linear Regression, Polynomial Features, Random Forest Regressor, K-Neighbors Regressor, Support Vector Regression, Ridge-Lasso Regression) were tested with R^2 (coefficient of determination) as a score metric. After comparison, Random Forest Regressor showed the best results.

For carbon increase model the best accuracy was obtained for input parameters Al_2O_3, MgO, $\ln(CaO/SiO_2)$, *Visc*, MgOS. For lining wear model the best accuracy was obtained for input parameters Al_2O_3, CaO, MgO, SiO_2, Visc. These results are given in **Fig. 11**.

The trained models were also used to predict the carbon increase in steel and lining wear in the range of input parameters, where no experiments were performed. For this purpose, the input parameters were generated by the «Space-filling Latin hypercube» method [33].

Both prediction models were implemented in a calculator that allows evaluating the lining wear and carbon increase in steel depending on the slag composition. The examples of calculation are presented in **Fig. 12**.

In addition to the graphical representation of the results, the calculator provides the chemical composition of the slag with the smallest carbon increase and with the lowest lining wear (**Table 5**).

Conclusions

In this work, we studied the interaction of slags with a high content of Al_2O_3 with a periclase-carbon lining in the smelting of dynamo steel. The obtained results can be summarized in a following way:

1. A relatively small change in the chemical composition of the slag can significantly vary its phase composition, and this is the main factor that affects the degree of slag corrosion of the periclase lining;

2. By using a slag with a certain phase composition, it is possible to obtain extremely small corrosion of the periclase lining, which is especially important in the conditions of ultra-low-carbon steels processing when using periclase-carbon lining as the slag line;

3. Spinel, formed as a result of the interaction of slags containing Al_2O_3 with the periclase of the lining, is not necessarily a protective layer by itself, but only acts in a combination with the properties of the oxide melt, which prevents the spinel from erosion and further contact of the slag and the lining

4. Calcium dialuminate $CaAl_4O_7$ acts in the slag composition as a protective phase for the periclase lining, which prevents the washing out of the corrosion products and further destruction of the refractory;

5. Based on the experiment results, predictive models for lining corrosion and metal carburization were developed. These models are based on the slag physical and chemical properties and can be used for the quick assessment of corrosion effects and carbon increase in the melt.

Our further research aims to determine the criteria for obtaining calcium aluminates in an oxide melt to reduce the corrosive effect of slag on the lining and the carbon content in steel.

Acknowledgments

This research did not receive any specific grant from funding agencies in the public, commercial, or not-for-profit sectors.

Declaration of competing interest

The authors declare that they have no known competing financial interests or personal relationships that could have appeared to influence the work reported in this paper.

Table 5. **Recommendations for slag compositions, which leads to the lowest carbon increase in steel and lining wear**

Al_2O_3	CaO	MgO	FeO	Visc_ini_Slag	SiO_2	B
23.08	42.14	12.0	15.0	0.0212	7.77	5.42

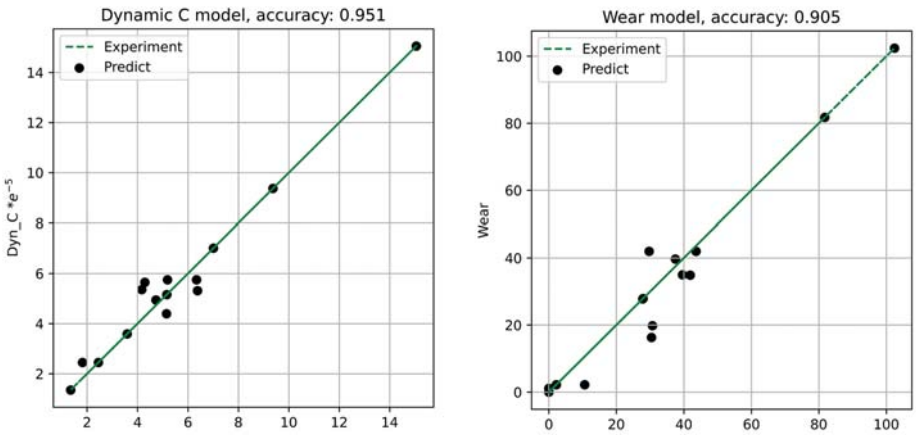

(*a*) (*b*)

Fig. 11. The results for all experiment points for: (*a*) carbon increase model, (*b*) lining wear model

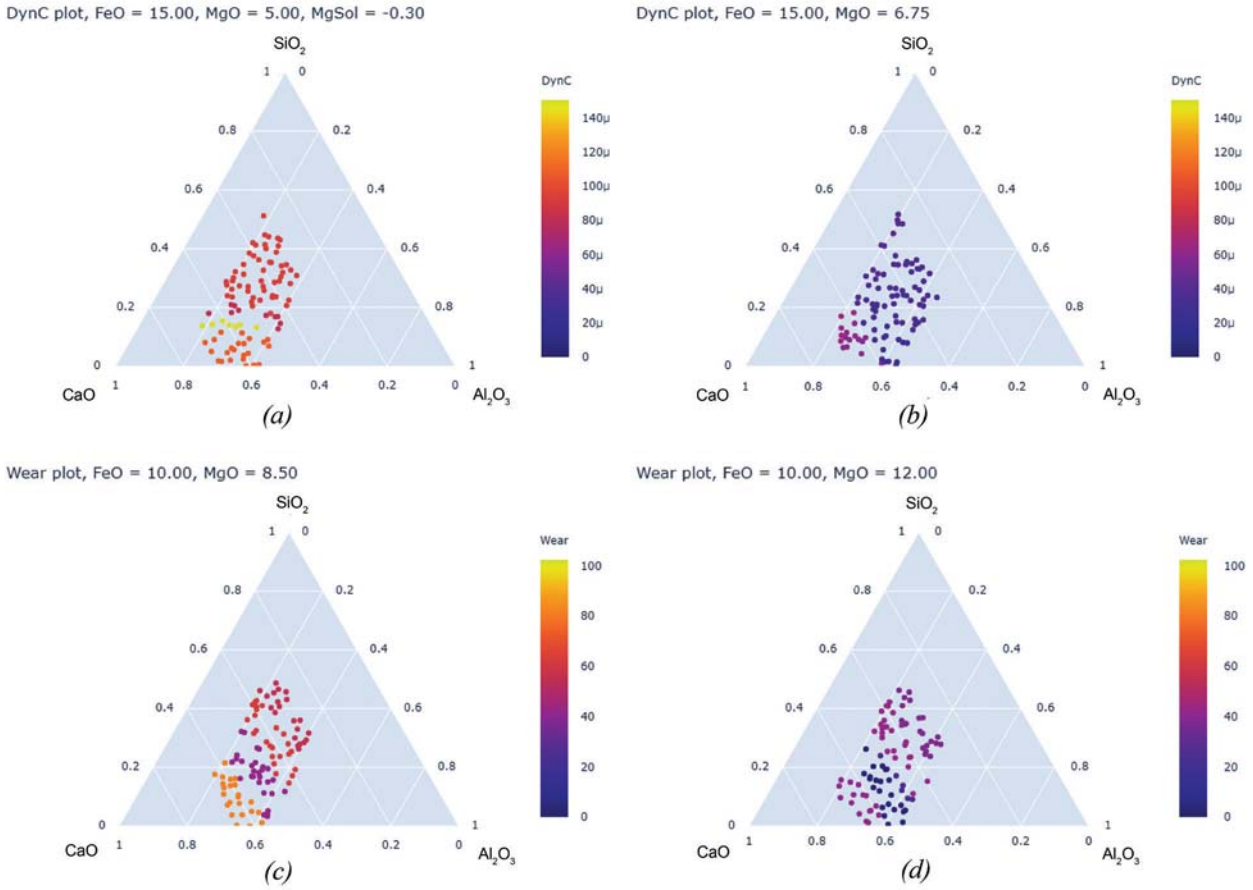

Fig. 12. Results of the forecast of carbon increase in steel and lining wear calculations

REFERENCES

1. Viertauer A., Mutsam N., Pernkopf F., Gantner A., Grimm G., Winkler W., Lammer G., Ratz A. Refractory condition monitoring and lifetime prognosis for Rh degasser. *AISTech – Iron and Steel Technology Conference Proceedings. May 2019*. 2019. pp. 1081–1089. DOI: 10.33313/377/111.
2. Guo M., Parada S., Jones P. T., Boydens E., Dyck J. V., Blanpain B., Wollants P. Interaction of Al_2O_3-rich slag with MgO–C refractories during VOD refining-MgO and spinel layer formation at the slag/refractory interface. *Journal of the European Ceramic Society*. 2009. No. 6 (29). pp. 1053–1060. DOI: 10.1016/j.jeurceramsoc.2008.07.063.
3. Wang D., Li X., Wang H., Mi Y., Jiang M., Zhang Y. Dissolution rate and mechanism of solid MgO particles in synthetic ladle slags. *Journal of Non-Crystalline Solids*. 2012. No. 9 (358). pp. 1196–1201. DOI: 10.1016/j.jnoncrysol.2012.02.014.
4. Nightingale S. A., Monaghan B. J. Kinetics of spinel formation and growth during dissolution of MgO in $CaO–Al_2O_3–SiO_2$ Slag. *Metallurgical and Materials Transactions B: Process Metallurgy and Materials Processing Science*. 2008. No. 5 (39). pp. 643–648. DOI: 10.1007/s11663-008-9186-y.
5. Xu L., Chen M., Wang N., Yin X. Corrosion mechanism of $MgAl_2O_4–CaAl_4O_7–CaAl_{12}O_{19}$ composite by steel ladle slag: Effect of additives. *Journal of the European Ceramic Society. 2017*. No. 7 (37). pp. 2737–2746. DOI: 10.1016/j.jeurceramsoc.2017.02.025.
6. Luz A. P., Leite F. C., Brito M. A. M., Pandolfelli V. C. Slag conditioning effects on MgO–C refractory corrosion performance. *Ceramics International*. 2013. No. 7 (39). pp. 7507–7515. DOI: 10.1016/j.ceramint.2013.03.001.
7. Rocha V. C. D., Alves P. C., Pereira J. A. M., Leal L. P., Bielefeldt W. V., Vilela A. C. F. Experimental and thermodynamic analysis of MgO saturation in the $CaO–SiO_2–Al_2O_3–MgO$ slag system melted in a laboratory resistive furnace. *Journal of Materials Research and Technology*. 2019. No. 1 (8). pp. 861–870. DOI: 10.1016/j.jmrt.2018.05.022.
8. Li X., Zhu B., Wang T. Effect of electromagnetic field on slag corrosion resistance of low carbon MgO–C refractories. *Ceramics International*. 2012. No. 3 (38). pp. 2105–2109. DOI: 10.1016/j.ceramint.2011.10.049.
9. Preisker T., Gehre P., Schmidt G., Aneziris C.G., Wöhrmeyer C., Parr C. Kinetics of the formation of protective slag layers on $MgO–MgAl_2O_4$–C ladle bricks determined in laboratory. *Ceramics International*. 2019. No. July. pp. 1–8. DOI: 10.1016/j.ceramint.2019.08.282.
10. Lee W. E., Zhang S. Direct and indirect slag corrosion of oxide and oxide-c refractories. *7th Int. Conference on Molten Slags Fluxes and Salts*. 2004. pp. 309–320.
11. Liu Y., Wang L., Li G., Zhang Z., Xu X., Li Y., Chen J. Effect of Submicron-Carbon-Containing MgO–C Refractories on Carbon Pickup of Ultra-Low Carbon Steel. *J. Ceram. Sci. Technol*. 2018. Vol. 9. Iss. 2. pp. 141–148.
12. Brabie V. A study on the mechanism of reaction between refractory materials and aluminium deoxidized molten steel. *Steel Research*. 1997. No. 2 (68). pp. 54–60. DOI: 10.1002/srin.199700542.
13. Park J. H., Min D. J. Solubility of carbon in $CaO–B_2O_3$ and $BaO–B_2O_3$ slags. Metallurgical and Materials Transactions B: Process *Metallurgy and Materials Processing Science*. 1999. No. 6 (30). pp. 1045–1052. DOI: 10.1007/s11663-999-0110-x.
14. Kuwata H. S. Solubility of Carbon in $CaO–Al_2O_3$ Melts. *Metallurgical and Materials Transactions B*. 1996. Vol. 27. No. 1. pp. 57–64.
15. Berryman R. A., Sommerville I. D. Carbon Solubility as Carbide in Calcium Silicate Melts. *Metallurgical and Materials Transactions B*. 1992. No. 23 (April). pp. 223–227.

16. Park J. H., Min D.J , Song H. S. Carbide Capacity of CaO–Al_2O_3–CaF_2 Slag at 1773 K. *ISIJ International*. 2002. No. 2 (42). pp. 127–131.
17. Park J. Y., Jung S. M., Sohn I. Carbon solubility in the CaO–SiO_2–3MgO–CaF_2 slag system. *Metallurgical and Materials Transactions B: Process Metallurgy and Materials Processing Science*. 2014. No. 2 (45). pp. 329–333. DOI: 10.1007/s11663-014-0028-9.
18. Sinelnikov V. O., Kalisz D., Kuzemko R. D. Study of the phase and mineralogical properties of converter slag during splashing to improve lining resistance. *Refractories and Industrial Ceramics*. 2018. No. 4 (59). pp. 403–409. DOI: 10.1007/s11148-018-0244-y.
19. Yuan Z., Wu Y., Zhao H., Matsuura H., Tsukihashi F. Wettability between molten slag and MgO–C refractories for the slag splashing process. *ISIJ International*. 2013. No. 4 (53). pp. 598–602. DOI: 10.2355/isijinternational.53.598.
20. Fu L., Gu H., Huang A., Zou Y., Ni H. Enhanced corrosion resistance through the introduction of fine pores : Role of nano-sized intracrystalline pores. *Corrosion Science*. 2019. No. 161 (August). pp. 108182. DOI: 10.1016/j.corsci.2019.108182.
21. Amini S., Brungs M., Jahanshahi S., Ostrovski O. Effects of additives and temperature on the dissolution rate and diffusivity of MgO in CaO–Al_2O_3 slags under forced convection. *ISIJ International*. 2006. No. 11 (46). pp. 1554–1559. DOI: 10.2355/isijinternational.46.1554.
22. Zou Y., Gu H., Huang A., Zhang M., Zhang M. Effects of aggregate microstructure on slag resistance of lightweight Al_2O_3–MgO castable. *Ceramics International*. 2017. No. 18 (43). pp. 16495–16501. DOI: 10.1016/j.ceramint.2017.09.033.
23. Svantesson J. L., Glaser B., Ersson M., White J. F., Jönsson P. G. Study of dynamic refractory wear by slags containing very high FeO contents under steelmaking conditions. *Ironmaking & Steelmaking*. 2021. Vol. 48. No. 5. pp. 607–618. DOI: 10.1080/03019233.2020.1827672.
24. Petkov V., Jones P. T., Boydens E., Blanpain B., Wollants P. Chemical corrosion mechanisms of magnesia – chromite and chrome-free refractory bricks by copper metal and anode slag. *Journal of the European Ceramic Society*. 2007. Vol. 27. pp. 2433–2444. DOI: 10.1016/j.jeurceramsoc.2006.08.020.
25. Sun S., Zhang L., Jahanshahi S. From viscosity and surface tension to marangoni flow in melts. *Metallurgical and Materials Transactions B*. 2003. No. 5 (34). pp. 517–523. DOI: 10.1007/s11663-003-0019-8.
26. Jeon J., Kang Y., Park J. H., Chung Y. Corrosion-erosion behavior of $MgAl_2O_4$ spinel refractory in contact with high MnO slag. *Ceramics International*. 2017. No. 17 (43). pp. 15074–15079. DOI: 10.1016/j.ceramint.2017.08.034.
27. Roduit N. JMicroVision: Image analysis toolbox for measuring and quantifying components of high-definition images. Version 1.3.4. Acceptable at: https://jmicrovision.github.io (reference date: 29.06.2021).
28. Bale C. W., Bélisle E., Chartrand P., Decterov S. A., Eriksson G., Hack K., Jung I. H., Kang Y. B., Melançon J., Pelton A. D., Robelin C., Petersen S. FactSage thermochemical software and databases - recent developments. *Calphad: Computer Coupling of Phase Diagrams and Thermochemistry*. 2009. No. 2 (33). pp. 295–311. DOI: 10.1016/j.calphad.2008.09.009.
29. Cho M. K., Hong G. G., Lee S. K. Corrosion of spinel clinker by CaO–Al_2O_3–SiO_2 ladle slag. *Journal of the European Ceramic Society*. 2002. No. 11 (22). pp. 1783–1790. DOI: 10.1016/S0955-2219(01)00509-X.
30. Xin Y. Lou, Yin H. F., Tang Y., Wan Q. F., Gao K., Yuan H. D., Wang Z. W. Formation mechanism and characterization of gradient density in corundum–spinel refractory. *Ceramics International*. 2019. No. 6 (45). pp. 8023–8026. DOI: 10.1016/j.ceramint.2018.12.199.
31. Saltelli A., Ratto M., Andres T., Campolongo F., Cariboni J., Gatelli D. Global Sensitivity Analysis: The Primer. International Statistical Review. Chichester (England): John Wiley & Sons, 2008. 304 p.
32. Pedregosa F., Varoquaux G., Gramfort A., Michel V., Thirion B., Grisel O., Blondel M., Prettenhofer P., Weiss R., Dubourg V., Vanderplas J., Passos A., Cournapeau D., Brucher M., Perrot M., Duchesnay É. Scikit-learn: Machine Learning in Python. *Journal of Machine Learning Research*. 2011. No. 85 (12). pp. 2825–2830.
33. Gramacy R. B. Surrogates: Gaussian Process Modeling, Design and Optimization for the Applied Sciences. Boca Raton, Florida: Chapman Hall/CRC, 2020. https://bookdown.org/rbg/surrogates/chap4.html (accessed February 22, 2021).